

## Fragment emission mechanism in the $^{32}\text{S} + ^{12}\text{C}$ reaction

Ratnesh Pandey,<sup>1,\*</sup> S. Kundu,<sup>1,2</sup> C. Bhattacharya,<sup>1,2</sup> K. Banerjee,<sup>1,2</sup> T. K. Rana,<sup>1</sup> S. Manna,<sup>1,2</sup> G. Mukherjee,<sup>1,2</sup> J. K. Meena,<sup>1</sup> A. Chaudhuri,<sup>1,2</sup> T. Roy,<sup>1,2</sup> Pratap Roy,<sup>1,2</sup> Md. A. Asgar,<sup>1,2</sup> V. Srivastava,<sup>1</sup> A. Dey,<sup>1</sup> M. Sinha,<sup>1</sup> T. K. Ghosh,<sup>1,2</sup> S. Bhattacharya,<sup>1</sup> S. K. Pandit,<sup>2,3</sup> K. Mahata,<sup>2,3</sup> P. Patle,<sup>3</sup> S. Pal,<sup>4</sup> A. Shrivastava,<sup>2,3</sup> and V. Nanal<sup>4</sup>

<sup>1</sup>Variable Energy Cyclotron Centre, 1/AF Bidhan Nagar, Kolkata - 700064, India

<sup>2</sup>Homi Bhabha National Institute, Training School Complex, Anushakti Nagar, Mumbai - 400094, India

<sup>3</sup>Nuclear Physics Division, Bhabha Atomic Research Centre, Mumbai - 400085, India

<sup>4</sup>Tata Institute of Fundamental Research, Mumbai - 400005, India

(Received 25 April 2017; published 5 June 2017)

The complex fragment emission from the decay of fully energy-relaxed composite,  $^{44}\text{Ti}^*$  formed via the  $^{32}\text{S} + ^{12}\text{C}$  reaction at two excitation energies, have been studied. Inclusive energy distributions of the fragments ( $3 \leq Z \leq 8$ ) emitted in the reaction  $^{32}\text{S} + ^{12}\text{C}$  have been measured in the angular range  $\sim 16^\circ\text{--}28^\circ$ , at two incident energies, 200 and 220 MeV, respectively. Damped fragment yields in all the cases have been found to have the characteristic of emission from fully-energy-equilibrated composites. The binary fragment yields are found to be in good agreement with the standard statistical model predictions of the extended Hauser–Feshbach model (EHFM).

DOI: 10.1103/PhysRevC.95.064603

### I. INTRODUCTION

For the last few decades, extensive studies [1–11] have been made to understand the fragment emission mechanisms for low-energy nucleus-nucleus collisions. These studies reveal that, for low energy ( $\leq 10$  MeV/u), light heavy-ion ( $A_{\text{proj}} + A_{\text{target}} \leq 60$ ) collisions, fusion followed by asymmetric fission (FF) [12–17] and deep inelastic orbiting [8–11] are two dominant mechanisms, which contribute to the observed fully energy damped yields of the fragments. It has been observed that deep inelastic orbiting mechanism [8–11] plays a significant role in fragment emission from the reactions involving  $\alpha$ -cluster nuclei (e.g.,  $^{20}\text{Ne} + ^{12}\text{C}$  [8,9],  $^{24}\text{Mg} + ^{12}\text{C}$  [18],  $^{28}\text{Si} + ^{12}\text{C}$  [19], etc.). In the deep inelastic orbiting process it is assumed that, instead of forming a compound nucleus (CN) as in FF process, a long-lived, dinuclear molecular complex [11] is formed with a strong memory of the entrance channel. In addition, in the case of the light heavy-ion systems, the shapes of the orbiting dinuclear systems are quite similar to the saddle and scission shapes obtained in the course of evolution of the FF process. Moreover, both orbiting and fusion-fission processes occur on similar timescales and hence the distinction between the signatures of the two processes is a real challenge. In spite of this, quite a few attempts have been made to differentiate these processes. In extensive studies for  $^{20}\text{Ne} + ^{12}\text{C}$  [20,21],  $^{16}\text{O} + ^{12}\text{C}$  [22] systems, it has been demonstrated that, even at higher bombarding energies, the signatures of equilibration persists, i.e., the most probable  $Q$  values for the fragments were found to be independent of detection angles and the resulting angular distributions of the fragments were found to have  $\sim 1/\sin\theta_{\text{c.m.}}$ -like angular dependence; However, the enhancement in the fully energy damped fragment yields near the entrance channel over the statistical model predictions, indicated the survival of orbiting at higher excitation energies. Since it is believed that orbiting is

associated with the formation of a highly deformed dinuclear configuration, the study of deformation of the hot composites using light charged particle (LCP) emission as a probe [23] can be used to differentiate between FF and orbiting processes. Survival of orbiting has further been established for the  $^{20}\text{Ne} + ^{12}\text{C}$  [24],  $^{16}\text{O} + ^{12}\text{C}$  [25],  $^{28}\text{Si} + ^{12}\text{C}$  [26] systems, where large deformations have been observed over the statistical model predictions by using LCP as a probe. So it will be interesting to investigate if orbiting continues to play significant role in heavier  $\alpha$ -cluster nuclei, too. In a detailed study of fragment emission from the compound system  $^{44}\text{Ti}$ , produced via the  $\alpha$ -cluster system  $^{32}\text{S} + ^{12}\text{C}$  at 280 MeV, Planeta *et al.* [27] established that fragments ( $7 \leq Z \leq 16$ ) were emitted due to symmetric splitting followed by evaporation. On the other hand, Oliveira *et al.* [28] have measured the energy-damped yield of binary fragments and quasi-elastic emission from the system  $^{28}\text{Si} + ^{16}\text{O}$ , which produces the same composite  $^{44}\text{Ti}$  at two different energies, viz.  $E_{\text{c.m.}} = 39.10$  and 50.5 MeV, respectively, and found that the  $Q$ -value-integrated angular distributions follows  $\sim 1/\sin\theta_{\text{c.m.}}$ -type behavior, indicating a long-lived intermediate state. However, the observation that the mass distributions peaks near to projectile and target mass, the ratio between the oxygen and carbon cross sections is rather large; and the total kinetic energy (TKE) values are significantly larger than the Coulomb repulsion, have conjectured the presence of the noncompound orbiting like mechanisms for the energy damped yield of the fragments from the system  $^{28}\text{Si} + ^{16}\text{O}$ . Moreover, a large deformation has also been observed in the study of LCP emission from the same composite  $^{44}\text{Ti}^*$  produced at different excitations via the reaction  $^{16}\text{O}$  (76, 96, 112 MeV) +  $^{28}\text{Si}$  [29]. The observation of large deformation may be associated with orbiting process. Hence, a more detailed study of this system is necessary to delineate the fragment emission mechanism. Since Planeta *et al.* [27] made a detailed study for the fragments having atomic numbers ( $7 \leq Z \leq 16$ ), it will, therefore, be worthwhile to study the emission of lighter fragments ( $Z \leq 6$ )

\*ratnesh@vecc.gov.in

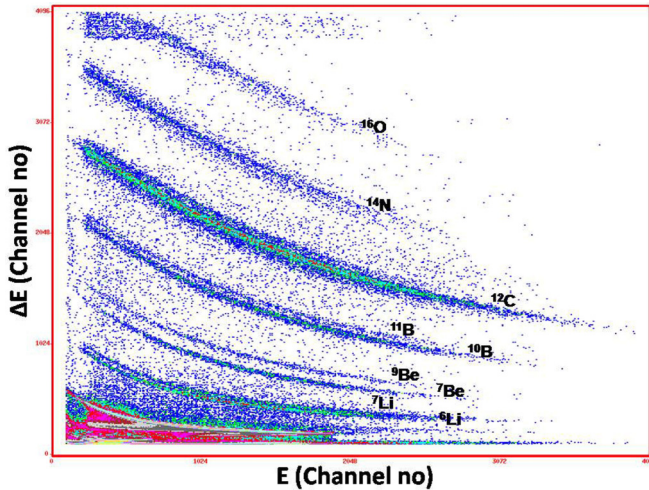


FIG. 1. Typical two-dimensional spectrum of fragments obtained in the reaction  $^{32}\text{S} + ^{12}\text{C}$ .

in particular, for the system  $^{44}\text{Ti}^*$  to extract the contributions of different emission processes. With this aim, we have studied and report here the light fragments ( $Z \leq 8$ ) emission from the same compound system  $^{44}\text{Ti}^*$  produced via the reaction  $^{32}\text{S} + ^{12}\text{C}$  at 200 and 220 MeV incident energies. The paper has been arranged as follows: The experimental arrangement is described in Sec. II, in brief. The experimental results are presented in Sec. III. In Sec. IV, theoretical analysis of the data is discussed in detail. Finally, the summary and conclusion are given in Sec. V.

## II. EXPERIMENTAL DETAILS

The experiment was performed by using 200 and 220 MeV  $^{32}\text{S} + ^{14}\text{C}$  from the BARC-TIFR Pelletron–Linac facility, Mumbai. The  $^{32}\text{S} + ^{14}\text{C}$  ion beam was bombarded on a self-supported  $^{12}\text{C}$  target of thickness  $\sim 390 \mu\text{g}/\text{cm}^2$  to produce the composite  $^{44}\text{Ti}^*$  at excitation energies ( $\sim 65$  MeV) and ( $\sim 71$  MeV), respectively. Different fragments ( $3 \leq Z \leq 8$ ) have been detected by using a three-element telescope, consisting of single-sided  $\sim 50\text{-}\mu\text{m}$ -thick Si ( $\Delta E$ ) strip detector (16 vertical strips of 3 mm width), followed by a double sided  $\sim 525\text{-}\mu\text{m}$ -thick Si(E) strip detector (16 strips, width 3 mm, both sides mutually orthogonal to each other) backed by four CsI(Tl) detectors, each of thickness 6 cm. The angular resolution was  $0.8^\circ$ . The solid angle covered by each detector were  $\sim 3$  msr. The isotopic separations obtained in this experiment are illustrated by the  $\Delta E$  vs  $E$  plot displayed in Fig. 1. Well separated ridges are clearly seen corresponding to elements having atomic numbers up to  $Z = 8$  and isotopic separation have been obtained for the fragments up to  $Z = 5$ . The inclusive energy distributions for various fragments ( $3 \leq Z \leq 8$ ) have been measured in the angular range of  $\sim 16^\circ$ – $28^\circ$  in the laboratory. This covered  $\sim 40^\circ$ – $80^\circ$  angles in the center-of-mass (c.m.) frame, because of the inverse kinematics of the reactions. A Versa–Module–Eurocard (VME) based online data-acquisition system LAMPS [30] was used for the collection of data on an event-by-event basis. Energy calibration of the telescope has

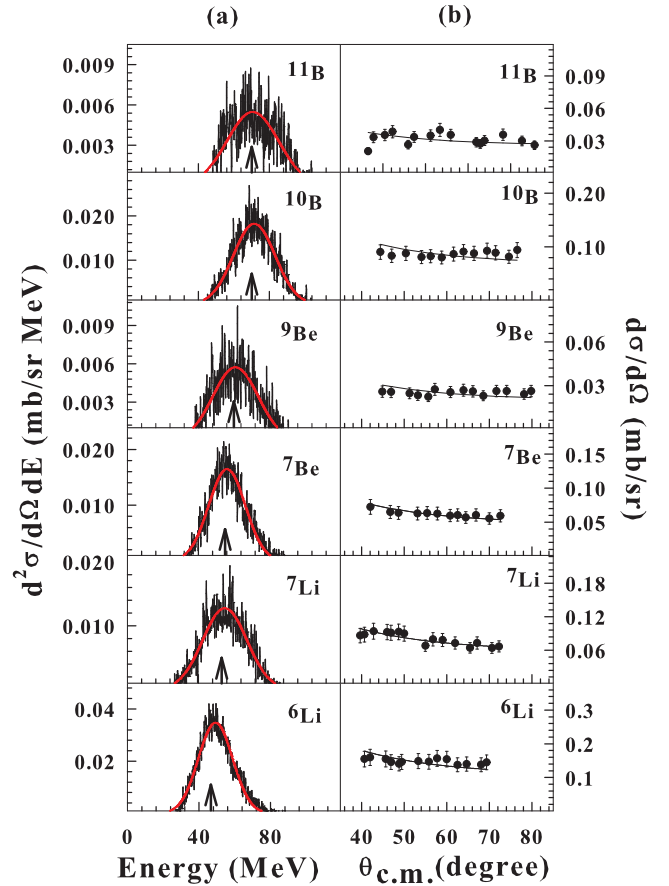


FIG. 2. (a) Isotopic energy distribution of fragments obtained from reaction  $^{32}\text{S}$  (220 MeV) +  $^{12}\text{C}$  at an angle  $\theta_{\text{lab}} = 21.6^\circ$ . Red solid line shows fitted Gaussian and arrow indicates the energy of the fragments as obtained from Viola systematics. (b) Isotopic angular distribution of fragments for the same reaction.

been done using the  $^{229}\text{Th}$  ( $\alpha$  source). The systematic errors in the data, arising from the uncertainties in the measurements of target thickness, solid angle and the calibration of current digitizer, have been estimated to be  $\sim 15\%$ .

## III. EXPERIMENTAL RESULTS

Typical energy spectra for different isotopes of the fragments ( $3 \leq Z \leq 5$ ) obtained at an angle of  $\sim 21.6^\circ$  at  $E_{\text{lab}} = 220$  MeV, is shown in Fig. 2(a). It is evident from Fig. 2(a) that energy spectra of isotopes of different ejectiles ( $3 \leq Z \leq 5$ ) at this bombarding energy exhibit strong peaking as a function of energy. Similar behavior has also been observed for the fragments emitted at bombarding energy  $E_{\text{lab}} = 200$  MeV. It has been observed that the energy distributions of isotopes of each fragment ( $3 \leq Z \leq 5$ ) are nearly Gaussian in shape at both the incident energies. The Gaussian fits so obtained are shown by solid lines in Fig. 2(a); the centroids (shown by arrows) are found to correspond to the expected kinetic energies for the fission fragments obtained from the Viola systematics [31] corrected by the corresponding asymmetry factors [32]. This suggests that the isotopes of the fragments are

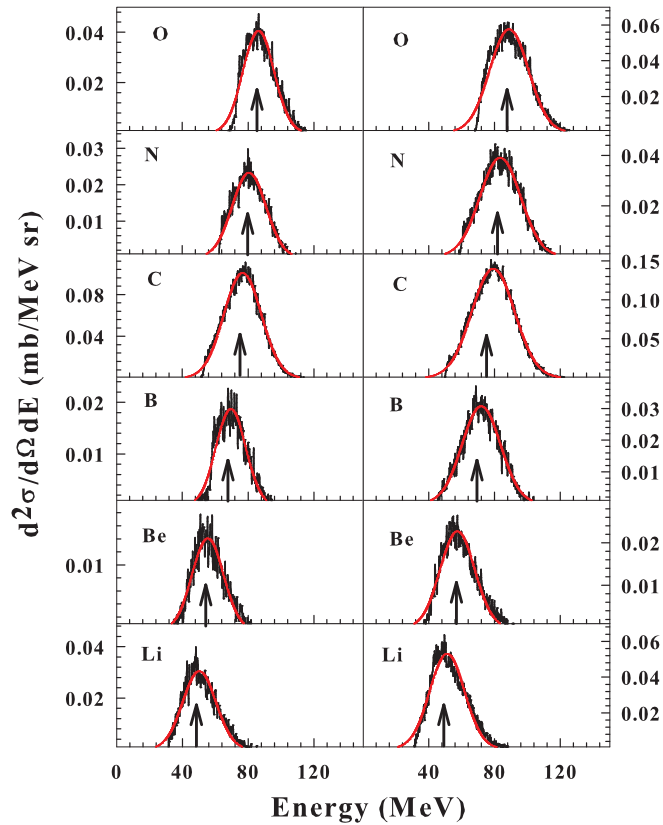


FIG. 3. Energy distribution of fragments for the reactions  $^{32}\text{S}$  (200, 220 MeV) +  $^{12}\text{C}$  at an angle  $\theta_{\text{lab}} = 21.6^\circ$ . Red solid line shows fitted Gaussian and arrow represents the energy of the fragments as obtained from Viola systematics.

emitted from a fully-energy-relaxed composite—as expected for both FF and orbiting processes. The angular distributions of isotopes of different fragments ( $3 \leq Z \leq 5$ ) in the laboratory have been obtained by integrating the corresponding Gaussian extracted from the energy distribution. The center-of-mass (c.m.) angular distributions of the isotopes of the fragments (Li, Be, and B) are shown in Fig. 2(b). It has been found that the angular distributions follow  $\sim 1/\sin\theta_{\text{c.m.}}$ -like variation (shown by solid lines), which further demonstrates that isotopes of these fragments are emitted from a fully energy relaxed, composite system. Since the energy and angular distributions of different isotopes of each fragments show similar behavior, so in the following we present the result of our elemental analysis instead of isotopic analysis.

#### A. Energy distribution

The energy spectra for various fragments Li, Be, B, C, N, and O ( $3 \leq Z \leq 8$ ) obtained at an angle  $21.6^\circ$  for incident energies  $E_{\text{lab}} = 200$  and 220 MeV are shown in the Fig. 3. It is evident from Fig. 3 that the energy spectra of all the fragments, obtained at both incident energies, are nearly Gaussian in shape, having their centroid at the expected kinetic energies for the fission fragments obtained from the Viola systematics corrected by the corresponding asymmetry factors [31,32],

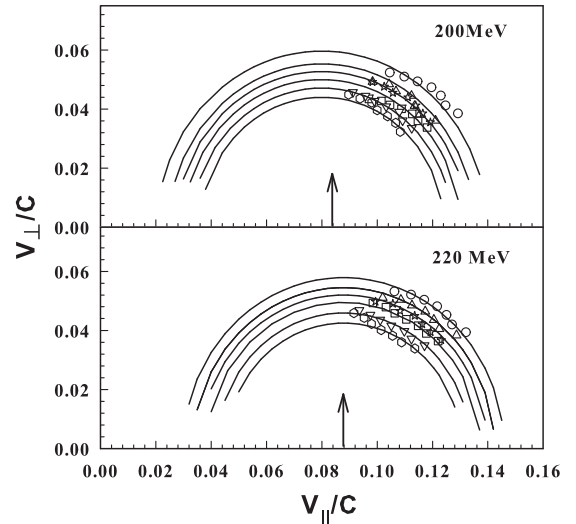


FIG. 4. The average velocities of the fragments plotted in  $v_{\parallel}$  vs  $v_{\perp}$  plane at bombarding energies 200 and 220 MeV. The average velocities are denoted by semi open circles (Li), open triangles (Be), open stars (B), open squares (C), open inverted triangles (N), and open hexagons (O). The arrows correspond to the compound nucleus velocities.

shown by solid arrows in Fig. 3. The Gaussian fits so obtained are shown by solid lines in Fig. 3.

#### B. Average velocity

The information about the degree of equilibration can be obtained if one plots the average velocities in  $v_{\parallel}$  vs  $v_{\perp}$  plane. The average velocities of the fragments have been obtained from the measured energies and from the  $Z$  values by using the empirical relation proposed by Charity *et al.* [33]:

$$A = Z(2.08 + 0.0029Z). \quad (1)$$

The average velocities of the fragments ( $3 \leq Z \leq 8$ ) obtained at incident energies  $E_{\text{lab}} = 200$  and 220 MeV, have been plotted in the  $v_{\parallel}$  vs  $v_{\perp}$  plane in Fig. 4. It is observed that, for both the incident energies, the average velocities of all the fragments fall on the circle centered around the respective  $v_{\text{CN}}$ , the compound-nuclear velocities, which indicates that, at both energies, the fragments are emitted from a fully equilibrated CN-like source with full momentum transfer. It also suggests that the average velocities (as well as kinetic energies) of the fragments are independent of the c.m. emission angles. The fact that the magnitude of the average fragment velocities (i.e., the radii of the circles in Fig. 4) decreases with the increase of fragment mass clearly confirms the binary nature of emission.

#### C. Angular distribution

The angular distributions of different fragments ( $3 \leq Z \leq 8$ ) in the laboratory frame have been obtained by integrating the corresponding Gaussian (Fig. 5) extracted from the energy distribution. The center-of-mass (c.m.) angular distributions of the fragments (Li, Be, B, C, N, and O), emitted in the  $^{32}\text{S}$  (200 and 220 MeV) +  $^{12}\text{C}$  reactions are shown in Fig. 5. The

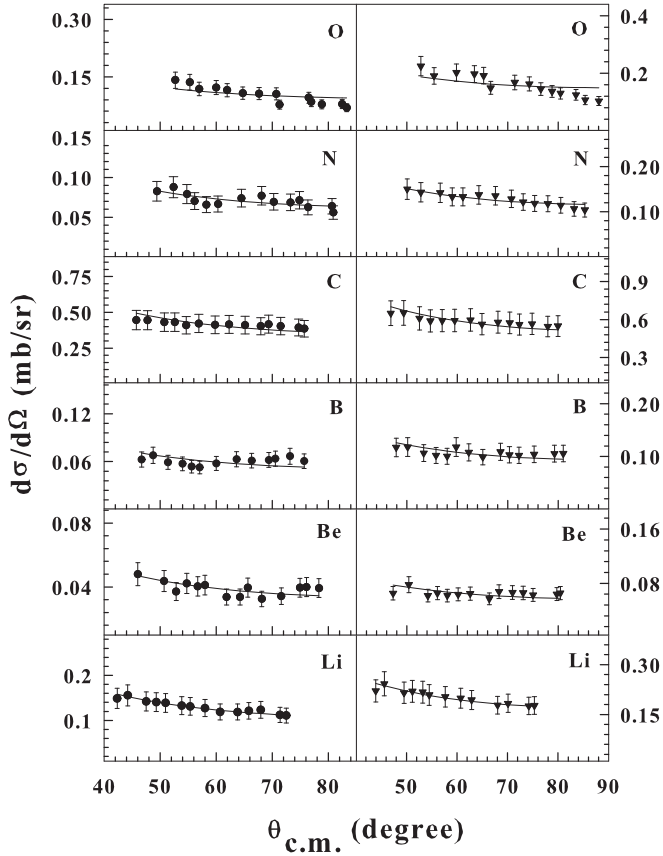


FIG. 5. Angular distribution of fragments obtained in the reaction  $^{32}\text{S} + ^{12}\text{C}$  at 200 and 220 MeV beam energy (denoted by circles and inverted triangles) as a function of c.m. angle.

transformations from the laboratory to c.m. system have been done with the assumption of a two-body kinematics averaged over a total-kinetic-energy distribution. It is observed that the c.m. angular distributions of these fragments obtained at both incident energies follow the  $\sim 1/\sin\theta_{\text{c.m.}}$ -like variation (shown by solid lines in Fig. 5), which further corroborates the conjecture of emission from fully equilibrated composite.

#### D. Average $Q$ -value distributions

The angular variation of the average  $Q$  values of the fragments also reflects on the degree of equilibration. The variations of average  $Q$  values,  $\langle Q \rangle$ , with c.m. emission angle for the fragments Li, Be, B, C, N, and O obtained at  $E_{\text{lab}} = 200$  and 220 MeV are shown in Fig. 6. It has been found that for all the fragments,  $\langle Q \rangle$  values are nearly constant and are independent of the c.m. emission angles for both the incident energies. Similar results have also been observed in the case of fragments emitted in  $^{20}\text{Ne} + ^{12}\text{C}$  [20,21] and  $^{16}\text{O} + ^{12}\text{C}$  [22] systems. However, this observation is totally different from those made earlier for the other lighter systems [ $^{16}\text{O}$  (116 MeV) +  $^{27}\text{Al}$ ,  $^{28}\text{Si}$ ,  $^{20}\text{Ne}$  (145, 158, 200, 218 MeV) +  $^{27}\text{Al}$ ], [2,3,34], for which a sharp falloff of  $\langle Q \rangle$  with c.m. emission angles have been seen. The constancy of  $\langle Q \rangle$  values with c.m. angles reveal the characteristics of fission like decay of an equilibrated composite system at both energies.

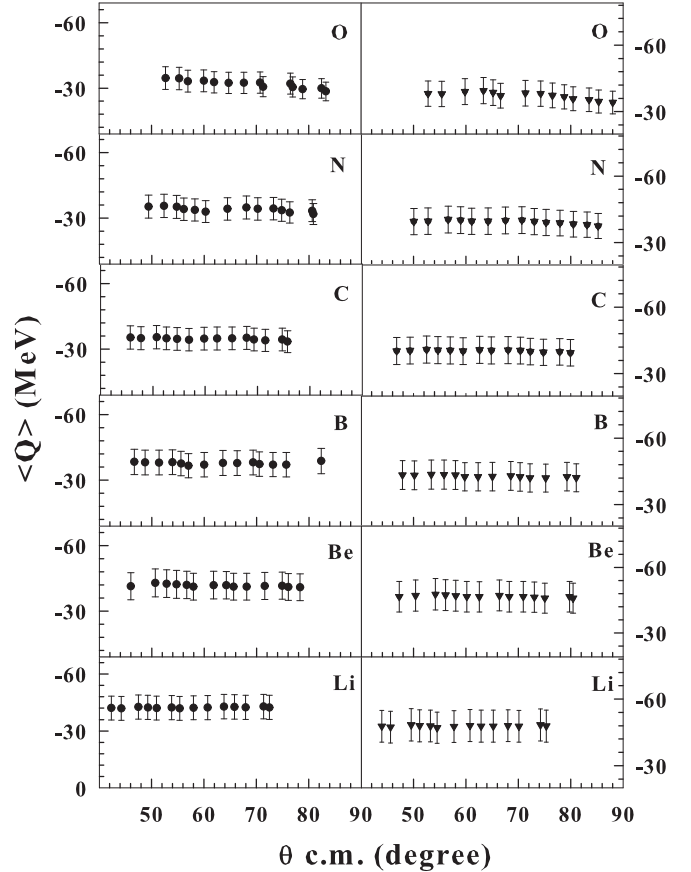


FIG. 6. Average  $\langle Q \rangle$  value of the fragments at 200 and 220 MeV incident energy (represented by circles and inverted triangles, respectively) plotted as a function of c.m. angle.

#### IV. CROSS SECTIONS

The experimental angle-integrated yields of the fragments emitted in the  $^{32}\text{S} + ^{12}\text{C}$  reaction at two bombarding energies are shown in Fig. 7 by solid circles. It is found that the yields of the fragments Li, Be, B, C, O, and N show similar behavior at both the incident energies; however, the cross section increases as the incident energy increases. The experimental FF fragment yields have been compared with the prediction obtained from the extended Hauser-Feshbach model (EHFM) [14] and are shown by histograms in Fig. 7. The values of the critical angular momenta have been obtained from the dynamical trajectory model calculations with realistic nucleus-nucleus interaction and the dissipative forces generated self-consistently through stochastic nucleon exchanges [35–37]. The values of the critical angular momentum  $l_{\text{cr}}$  for the system  $^{32}\text{S} + ^{12}\text{C}$  have been estimated to be  $(27\hbar)$  and  $(32\hbar)$  at 200 and 220 MeV, respectively. It is seen that, at both the incident energies, the theoretical predictions are in fair agreement with the experimental results.

#### V. DISCUSSION

In the case of the decay of  $^{44}\text{Ti}$ , produced via the  $\alpha$ -cluster system  $^{32}\text{S} + ^{12}\text{C}$  at 280 MeV, Planeta *et al.* [27] have shown that the measured fragment yields ( $7 \leq Z \leq 16$ ) were due

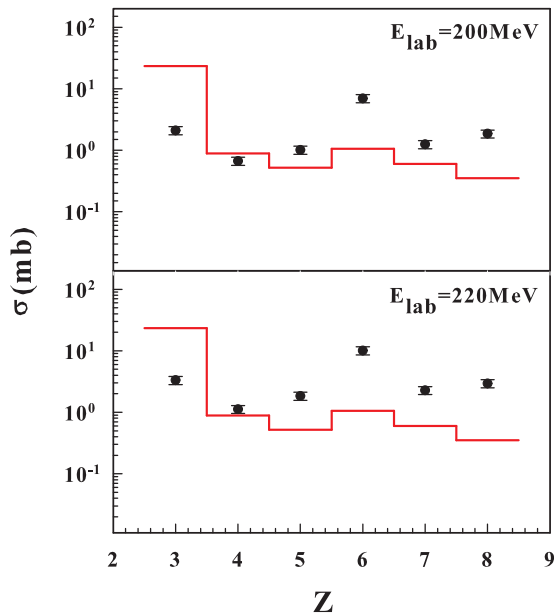


FIG. 7. Total cross section of different fragments obtained at incident energies 200 and 220 MeV. Red line represents corresponding EHF result.

to symmetric splitting of CN followed by evaporation. On the other hand, Oliveira *et al.* [28] have studied the energy-damped yield of binary fragments and quasi-elastic emission from the system  $^{28}\text{Si} + ^{16}\text{O}$ , which produces the same composite  $^{44}\text{Ti}$  at two different excitations, and concluded the presence of noncompound orbiting process and found the ratio between the oxygen and carbon cross sections is quite large. Moreover, the observation of large deformation in the study of light charged particle (LCP) emission from the same composite  $^{44}\text{Ti}^*$  produced via the reactions  $^{16}\text{O}$  (76, 96, 112 MeV) +  $^{28}\text{Si}$  [29] may be associated with the orbiting process. In the case of the light heavy-ion systems, the shapes of the orbiting dinuclear complexes are quite similar to the saddle and scission shapes obtained in the course of evolution of the FF process. Moreover, orbiting and fusion-fission processes occur on similar timescales, which makes it difficult to differentiate the signatures of the two processes. Study of entrance channel dependence may help in delineating these two processes. Absence of any entrance channel dependence will establish the compound-nuclear origin of the emission process. In the present study, the light fragments ( $Z \leq 8$ ) emission from the same compound system  $^{44}\text{Ti}^*$  produced via the reaction  $^{32}\text{S} + ^{12}\text{C}$  at 200 and 220 MeV incident energies have been studied. The fact that the energy distributions, velocity distributions, angular distributions, and  $\langle Q \rangle$  distributions, reflect that the yield of these fragments ( $3 \leq Z \leq 8$ ) originate from fully-energy-relaxed events associated with the decay of either compound nucleus or a long-lived, orbiting dinuclear system. A detailed investigation has been made to decipher the role played by the two aforementioned processes in the fragment yield by comparing the binary-reaction yields obtained from the same compound system  $^{44}\text{Ti}^*$  produced via a different entrance channel  $^{16}\text{O} + ^{28}\text{Si}$  [2,3] at little higher excitation

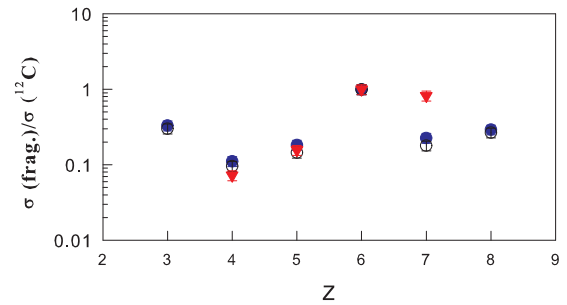


FIG. 8. Cross-section ratio vs Z plot of  $^{32}\text{S}$  (220 MeV) +  $^{12}\text{C}$ ,  $^{32}\text{S}$  (200 MeV) +  $^{12}\text{C}$ , and  $^{16}\text{O}$  (116 MeV) +  $^{28}\text{Si}$  reaction (represented by filled blue circles, open black circles, and red triangles, respectively).

energy. In Fig. 8, ratio of fragment yield obtained with respect to the fragment carbon have been shown for the reactions  $^{32}\text{S} + ^{12}\text{C}$  at 200 and 220 MeV incident energies by solid circles and empty circles, respectively, and for the reaction  $^{16}\text{O} + ^{28}\text{Si}$  are shown by triangles. It is seen that except for nitrogen, for all the fragments, the yield of elemental ratio obtained in three reactions are nearly same, clearly indicating compound-nuclear origin of these fragments. In the case nitrogen, the yield ratio obtained in  $^{16}\text{O} + ^{28}\text{Si}$  is slightly different, which may be due to contamination from deep-inelastic process in the forward-angle data [2,3]. The absence of any entrance channel dependence clearly confirms their emission from compound-nucleus origin.

The ratio between the experimental cross sections of oxygen and carbon fragment emission is shown in Fig. 9 as a function of the excitation energy. The  $^{16}\text{O}/^{12}\text{C}$  ratios are found to be same at all excitations and there is no such enhancement in the yield of  $^{16}\text{O}$  as observed in case of  $^{28}\text{Si} + ^{16}\text{O}$  reaction studied by Ref. [28]. This further corroborates the fact the energy damped yields of the fragments observed in the present reactions  $^{32}\text{S} + ^{12}\text{C}$  at 200 and 220 MeV incident energies are of compound-nuclear origin rather than the orbiting process as claimed by Ref. [28] for the reaction  $^{28}\text{Si} + ^{16}\text{O}$ .

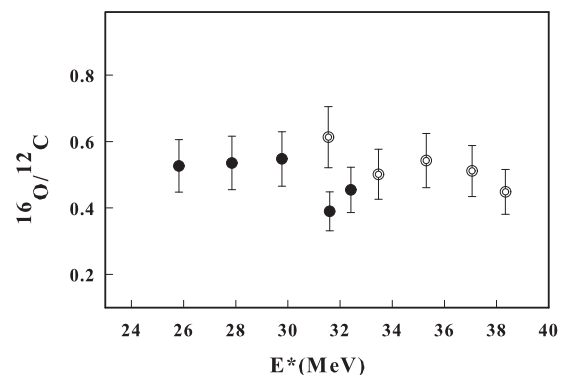


FIG. 9. Ratio of oxygen and carbon yield as a function of excitation energy, the filled and empty circles represents  $E_{\text{lab}} = 200$  and 220 MeV, respectively.

## VI. SUMMARY

The inclusive double-differential cross section for fragments ( $3 \leq Z \leq 8$ ) emitted in the reaction  $^{32}\text{S} + ^{12}\text{C}$  at the energies of 200 and 220 MeV have been measured in the angular range  $\sim 16^\circ\text{--}28^\circ$ . The energy distributions of all the fragments obtained at both incident energies, were found to be nearly Gaussian in shapes with their centroids at the expected kinetic energies for the binary break up obtained from the Viola systematics corrected by the corresponding asymmetric factors. The c.m. angular distributions of the fragments ( $3 \leq Z \leq 8$ ) obtained at both incident energies are found to follow  $\sim 1/\sin\theta_{\text{c.m.}}$  type of dependence, which conjectures the emission of these fragments from a long-lived equilibrated composite. The average velocity plots in  $v_{\parallel}$  vs  $v_{\perp}$  plane obtained at both incident energies indicated that, for all the fragments, average velocities fall on circle centered around the respective  $v_{\text{CN}}$ , compound-nuclear velocities, which corroborate that, at both incident energies, the fragments are emitted from fully equilibrated CN-like source with full momentum transfer. These observations also suggest that the average velocities (as well as kinetic energies) of the fragments are independent of the c.m. emission angles. The magnitude of the average fragment velocities (i.e., the radii of the circles in Fig. 4) were found to decrease with the increase of fragment mass, clearly indicating the binary nature of emission. It has also been observed that, for each fragments, at both

the incident bombarding energies, the average  $Q$  values are independent of emission angle, which further suggests that the fragments are emitted from a completely equilibrated source. The total elemental cross sections for different fragments ( $3 \leq Z \leq 8$ ) have been found to be in good agreement with the theoretical predictions of EHFM calculations, which supports the compound-nuclear origin of the emission process. The fact that there is no entrance channel dependence further substantiates the compound-nuclear origin of these fragments as observed by Planeta *et al.* [27] at higher excitation energy. Moreover, the  $^{16}\text{O}/^{12}\text{C}$  ratios are found to be same at all excitations and no significant enhancement has been observed in the yield of  $^{16}\text{O}$  as observed in case of the  $^{28}\text{Si} + ^{16}\text{O}$  reaction studied by Ref. [28]. This further substantiates the fact that the energy-damped yields of the fragments observed in the present reaction  $^{32}\text{S} + ^{12}\text{C}$  at 200 and 220 MeV incident energies are of compound-nuclear origin rather than the orbiting process as claimed by Ref. [28] for the reaction  $^{28}\text{Si} + ^{16}\text{O}$ .

## ACKNOWLEDGMENTS

The authors are thankful to the operating staff of the Pelletron–Linac facility for the smooth running of the machine during the experiment. One of the authors (S.B.) acknowledges with thanks the financial support received as Raja Ramanna Fellow from the Department of Atomic Energy, Government of India.

- 
- [1] S. J. Sanders, A. S. d. Toledo, and C. Beck, *Phys. Rep.* **311**, 487 (1999).
- [2] C. Bhattacharya, K. Mullick, S. Bhattacharya, K. Krishan, T. Bhattacharjee, P. Das, S. R. Banerjee, D. N. Basu, A. Ray, S. K. Basu, and M. B. Chatterjee, *Phys. Rev. C* **66**, 047601 (2002).
- [3] C. Bhattacharya, S. Bhattacharya, T. Bhattacharjee, A. Dey, S. Kundu, S. R. Banerjee, P. Das, S. K. Basu, and K. Krishan, *Phys. Rev. C* **69**, 024607 (2004).
- [4] C. Bhattacharya, D. Bandyopadhyay, S. K. Basu, S. Bhattacharya, K. Krishan, G. S. N. Murthy, A. Chatterjee, S. Kailas, and P. Singh, *Phys. Rev. C* **54**, 3099 (1996).
- [5] C. Beck *et al.*, *Eur. Phys. J. A* **2**, 281 (1998).
- [6] C. Beck, D. Mahboub, R. Nouicer, T. Matsuse, B. Djerroud, R. M. Freeman, F. Haas, A. Hachem, A. Morsad, M. Youlal, S. J. Sanders, R. Dayras, J. P. Wieleczko, E. Berthoumieux, R. Legrain, E. Pollacco, S. Cavallaro, E. De Filippo, G. Lanzańo, A. Pagano, and M. L. Sperduto, *Phys. Rev. C* **54**, 227 (1996).
- [7] K. A. Farrar, S. J. Sanders, A. K. Dummer, A. T. Hasan, F. W. Prosser, B. B. Back, I. G. Bearden, R. R. Betts, M. P. Carpenter, B. Crowell, M. Freer, D. J. Henderson, R. V. F. Janssens, T. L. Khoo, T. Lauritsen, Y. Liang, D. Nisius, A. H. Wuosmaa, C. Beck, R. M. Freeman, S. Cavallaro, and A. S. d. Toledo, *Phys. Rev. C* **54**, 1249 (1996).
- [8] D. Shapira, J. L. C. Ford, Jr., J. G. d. Campo, R. G. Stokstad and R. M. DeVries, *Phys. Rev. Lett.* **43**, 1781 (1979).
- [9] D. Shapira, J. L. C. Ford, Jr., and J. G. d. Campo, *Phys. Rev. C* **26**, 2470 (1982).
- [10] D. Shapira, R. Novotny, Y. C. Chan, K. A. Erb, J. L. C. Ford jr., J. C. Peng, and J. D. Moses, *Phys. Lett. B* **114**, 111 (1982).
- [11] B. Shivakumar, S. Ayik, B. A. Harmon, and D. Shapira, *Phys. Rev. C* **35**, 1730 (1987).
- [12] L. G. Moretto, *Nucl. Phys. A* **247**, 211 (1975).
- [13] S. J. Sanders, *Phys. Rev. C* **44**, 2676 (1991).
- [14] T. Matsuse, C. Beck, R. Nouicer, and D. Mahboub, *Phys. Rev. C* **55**, 1380 (1997).
- [15] A. K. Dhara, C. Bhattacharya, S. Bhattacharya, and K. Krishan, *Phys. Rev. C* **48**, 1910 (1993).
- [16] A. S. d. Toledo, S. J. Sanders, and C. Beck, *Phys. Rev. C* **56**, 558 (1997).
- [17] A. S. d. Toledo, B. V. Carlson, C. Beck, and M. Thoennessen, *Phys. Rev. C* **54**, 3290 (1996).
- [18] W. Dünneber, A. Glaesner, W. Hering, D. Konnerth, R. Ritzka, W. Trombik, J. Czakański, and W. Zipper, *Phys. Rev. Lett.* **61**, 927 (1988).
- [19] D. Shapira, D. Schull, J. L. C. Ford, Jr., B. Shivakumar, R. L. Parks, R. A. Cecil, and S. T. Thornton, *Phys. Rev. Lett.* **53**, 1634 (1984).
- [20] C. Bhattacharya, A. Dey, S. Kundu, K. Banerjee, S. Bhattacharya, S. Mukhopadhyay, D. Gupta, T. Bhattacharjee, S. R. Banerjee, S. Bhattacharyya, T. Rana, S. K. Basu, R. Saha, S. Bhattacharjee, K. Krishan, A. Mukherjee, D. Bandopadhyay, and C. Beck, *Phys. Rev. C* **72**, 021601(R) (2005).
- [21] A. Dey, C. Bhattacharya, S. Bhattacharya, S. Kundu, K. Banerjee, S. Mukhopadhyay, D. Gupta, T. Bhattacharjee, S. R. Banerjee, S. Bhattacharyya, T. K. Rana, S. K. Basu, R. Saha, K. Krishan, A. Mukherjee, D. Bandopadhyay, and C. Beck, *Phys. Rev. C* **76**, 034608 (2007).

- [22] S. Kundu, A. Dey, K. Banerjee, T. K. Rana, S. Mukhopadhyay, D. Gupta, R. Saha, S. Bhattacharya, and C. Bhattacharya, *Phys. Rev. C* **78**, 044601 (2008).
- [23] C. Beck, M. Rousseau, P. Papka *et al.*, APH N. S., Heavy Ion Physics 18/2-4, 297 (2003).
- [24] A. Dey, S. Bhattacharya, C. Bhattacharya, K. Banerjee, T. K. Rana, S. Kundu, S. Mukhopadhyay, D. Gupta, and R. Saha, *Phys. Rev. C* **74**, 044605 (2006).
- [25] S. Kundu, C. Bhattacharya, S. Bhattacharya, T. K. Rana, K. Banerjee, S. Mukhopadhyay, D. Gupta, A. Dey, and R. Saha, *Phys. Rev. C* **87**, 024602 (2013).
- [26] M. Rousseau, C. Beck, C. Bhattacharya, V. Rauch, O. Dorvaux, K. Eddahbi, C. Enaux, R. M. Freeman, F. Haas, D. Mahboub, R. Nouicer, P. Papka, O. Stezowski, S. Szilner, A. Hachem, E. Martin, S. J. Sanders, A. K. Dummer, and A. Szanto de Toledo, *Phys. Rev. C* **66**, 034612 (2002).
- [27] R. Płaneta, P. Belery, J. Brzywczyk, P. Cohilis, Y. E. Masri, G. Grégoire, K. Grotowski, Z. Majka, S. Micek, M. Szczodrak, A. Wieloch, and J. Albiński, *Phys. Rev. C* **34**, 512 (1986).
- [28] J. M. Oliveira, Jr., A. Lépine-Szily, A. C. C. Villari, R. Lichtenthäler, L. C. Gomes, W. Sciani, P. Fachini, G. L. Lima, A. C. G. Martins, V. Chiste, J. M. Casandjian, A. J. Pacheco, J. E. Testoni, D. Abriola, A. O. Macchiavelli, F. Hasenbalg, O. A. Capurro, D. Tomasi, J. F. Niello, and D. Brandizzi, *Phys. Rev. C* **53**, 2926 (1996).
- [29] P. Papka *et al.*, Acta Phys. Pol. B **34**, 2343 (2003); Ph.D. thesis, IReS and Université Louis Pasteur Strasbourg, 2003 (unpublished).
- [30] <http://www.tifr.res.in/pell/lamps.html>
- [31] V. E. Viola, K. Kwiatkowski, and M. Walker, *Phys. Rev. C* **31**, 1550 (1985).
- [32] C. Beck and A. S. d. Toledo, *Phys. Rev. C* **53**, 1989 (1996).
- [33] R. J. Charity, D. R. Bowman, Z. H. Liu, R. J. McDonald, M. A. McMahan, G. J. Wozniak, L. G. Moretto, S. Bradley, W. L. Kehoe, and A. C. Mignerey, *Nucl. Phys. A* **476**, 516 (1988).
- [34] A. Dey, C. Bhattacharya, S. Bhattacharya, T. K. Rana, S. Kundu, K. Banerjee, S. Mukhopadhyay, S. R. Banerjee, D. Gupta, and R. Saha, *Phys. Rev. C* **75**, 064606 (2007).
- [35] S. Bhattacharya, K. Krishan, S. K. Samaddar, and J. N. De, *Phys. Rev. C* **37**, 2916 (1988).
- [36] J. G. d. Campo and R. G. Stokstad, LILITA, a Monte Carlo Hauser-Feshbach code, ORNL-TM 7295.
- [37] W. D. M. Rae, A. J. Cole, B. G. Harvey, and R. G. Stokstad, *Phys. Rev. C* **30**, 158 (1984).